Fuzzy-Neural Sliding Mode Control of Uncertain Systems: A Lyapunov Theory Approach

ECS-9819310

Stanislaw H. Żak

School of Electrical and Computer Engineering

Purdue University

West Lafayette, IN 47907

Progress Report of the First Stage of the 3-Year Project

for

Dr. Radhakisan S. Baheti

Program Director
Control, Networks, and Computational Intelligence

1 Introduction

It had been stated in the proposal that the objectives of the proffered 3-year research effort was to incorporate neural networks, fuzzy systems and genetic algorithms into the design of sliding mode controllers, sliding mode state estimators and sliding mode identifiers of uncertain or nonlinear dynamical systems. In practice, the controller, as well as the plant, is subject to various nonlinear constraints like hard bounds on gains, limited energy, or finite switching speeds that must be taken into account in a realistic controller design. In addition, due to lack of knowledge of parameter values or inaccuracies in the modeling process, the designer must cope with uncertainties in the plant model. In this project, a deterministic approach to the control, identification and state estimation of uncertain dynamical systems has been taken. The plan is to provide a paradigm for fuzzy modeling that allows for systematic construction of fuzzy models for the purpose of the controllers' and state estimators' design. Adaptation algorithms for continuous-time sliding mode neural identifiers are currently being studied and novel variable structure sliding mode fuzzy controllers and state estimators are being developed. The proposed structures will be integrated into self-organizing fuzzy-neural sliding mode tracking controllers. The controllers' and state estimators' stability and their guaranteed performance will be analyzed and then tested on a simulation model of a ground vehicle. This vehicle model is suitable for the evaluation of the vehicle dynamical behavior in real-time. Optimization of the controllers' and estimators' parameters will be achieved using genetic algorithms. Neural network and fuzzy logic controllers have been used with considerable success in closed-loop applications. However, these applications, though very successful, have no proofs of guaranteed stability for uncertain systems with control variables limited in amplitude. In the proposed research, the direct method of Lyapunov, Hahn's extensions of the Lyapunov method and LaSalle's Invariance Principle are being used in the stability and guaranteed performance analyses of fuzzy-neural sliding mode control and identification structures. The results of the proposed research will contribute to the basic control theory as well as to the intelligent vehicle control systems.

The beginning date of this 3-year project was September 9, 1999. The first stage of

the project is the period between September 9, 1999 and August 8, 2000. The research effort during the first stage of the project was focused on three areas. The first area is the investigation of discrete-time variable structure sliding mode control and its applications to control uncertain dynamical systems. The second area of our research effort is modeling and fuzzy control of an antilock braking system which is a part of the vehicle model that we are developing as the test bed for our controllers. Finally, the third area of our research effort is devoted to fuzzy adaptive robust tracking controllers for uncertain systems. We now describe, in more detail, our research activities in each of the above mentioned areas.

2 Discrete-Time Variable Structure Control

A variable structure system (VSS) is a dynamical system whose structure changes in accordance with the current value of its state. A VSS can be viewed as a system composed of independent structures together with a switching logic to switch between the structures. To obtain high performance in a closed-loop system, a sliding mode is deliberately induced via appropriate switching logic to exploit the desirable properties of the components of the system [21, 22]. Furthermore, a VSS may have properties that do not belong to any of its structures. Sliding mode is the motion of a dynamical system's trajectory while confined to a surface chosen by a designer. Once in sliding mode, the system exhibits an order reduction which can be effectively used in the design of variable structure sliding mode controllers, which consists of two phases. They are: the construction of the switching (sliding) surface designed to achieve the desired system behavior, such as stability to the origin when restricted to the surface, and the selection of feedback gains of the controller so that the closed-system is stable to the sliding surface.

We distinguish among the continuous-time variable structure sliding mode (VSSM) control, sampled-data VSSM control, and discrete-time VSSM control. In our research activity in this stage, we focus on the discrete-time VSSM control which is the subject of a number of recent papers—see, for example, [16], [18], [14], [6], [28], [19], [27], [23], [17], [7], [20], [26],

among others. In 1989, Kotta [10] noticed that unlike in the continuous-time VSSM control, the control in the discrete-time case must be upper and lower bounded to guarantee that the switching surface is attractive. Furthermore, as the state trajectory approaches the switching manifold, these bounds approach each other and for the system in sliding the bounds are equal. This observation impelled Kotta [10] to raise the question about applicability of discrete-time variable structure sliding mode control.

We studied the differences in the requirements for the sliding mode behavior for continuous and discrete-time systems and investigated the limitations of discrete-time variable structure sliding mode control. The results of our findings were published in [9].

We considered discrete-time dynamical system models of the form

$$\boldsymbol{x}_{k+1} = \boldsymbol{A}\boldsymbol{x}_k + \boldsymbol{B}\boldsymbol{u}_k + \boldsymbol{d}_k, \tag{1}$$

where $\boldsymbol{x}_k \in \mathbb{R}^n$, $\boldsymbol{u}_k \in \mathbb{R}^m$, and rank $\boldsymbol{B} = m$, and the vector $\boldsymbol{d}_k$ models the uncertainties of the system model. As we mentioned above, the main feature of a variable structure controller is the switching surface. We considered linear switching surfaces of the form

$$\boldsymbol{\sigma}(\boldsymbol{x}) = \boldsymbol{S}\boldsymbol{x} = \boldsymbol{0}, \tag{2}$$

where $\boldsymbol{S} \in \mathbb{R}^{m\times n}$ is chosen so that the matrix $\boldsymbol{SB}$ is invertible. For the case when $\boldsymbol{d}_k = \boldsymbol{0}$, we have

$$\begin{aligned}
\boldsymbol{\sigma}_{k+1} &= \boldsymbol{S}\boldsymbol{x}_{k+1} \\
&= \boldsymbol{S}\left(\boldsymbol{A}\boldsymbol{x}_k + \boldsymbol{B}\boldsymbol{u}_k\right) \\
&= \left(\boldsymbol{SB}\right)\left(\left(\boldsymbol{SB}\right)^{-1}\boldsymbol{SA}\boldsymbol{x}_k + \boldsymbol{u}_k\right) \\
&= \left(\boldsymbol{SB}\right)\left(\boldsymbol{u}_k - \boldsymbol{u}_{eq,k}\right),
\end{aligned} \tag{3}$$

where

$$\boldsymbol{u}_{eq,k} = -\left(\boldsymbol{SB}\right)^{-1}\boldsymbol{SA}\boldsymbol{x}_k, \tag{4}$$

and is called the equivalent control. In sliding mode along (2), we need

$$\boldsymbol{\sigma}_k = \boldsymbol{\sigma}\left(\boldsymbol{x}_k\right) = \boldsymbol{0}. \tag{5}$$

Note that $\|\boldsymbol{\sigma}_k\|$ is a constant multiple of the distance of $\boldsymbol{x}_k$ to the switching surface. It is clear that $\boldsymbol{x}_{k+1}$ is on the switching surface if and only if $\boldsymbol{u}_k = \boldsymbol{u}_{eq,k}$.

We now compare the above with its continuous-time counterpart. Suppose that the system model is

$$\dot{\boldsymbol{x}}(t) = \boldsymbol{A}\boldsymbol{x}(t) + \boldsymbol{B}\boldsymbol{u}(t). \tag{6}$$

Let $\boldsymbol{\sigma}(t) = \boldsymbol{S}\boldsymbol{x}(t)$. Then, we have

$$\begin{aligned} \dot{\boldsymbol{\sigma}}(t) &= \boldsymbol{S}\dot{\boldsymbol{x}}(t) \\ &= \boldsymbol{S}\boldsymbol{A}\boldsymbol{x}(t) + \boldsymbol{S}\boldsymbol{B}\boldsymbol{u}(t) \\ &= (\boldsymbol{S}\boldsymbol{B})\left((\boldsymbol{S}\boldsymbol{B})^{-1}\boldsymbol{S}\boldsymbol{A}\boldsymbol{x}(t) + \boldsymbol{u}(t)\right) \\ &= (\boldsymbol{S}\boldsymbol{B})\left(\boldsymbol{u}(t) - \boldsymbol{u}_{eq}(t)\right), \end{aligned} \tag{7}$$

where $\boldsymbol{u}_{eq}(t) = -(\boldsymbol{S}\boldsymbol{B})^{-1}\boldsymbol{S}\boldsymbol{A}\boldsymbol{x}(t)$. Hence, $\dot{\boldsymbol{\sigma}}(t) = \boldsymbol{0}$ if and only if $\boldsymbol{u}(t) = \boldsymbol{u}_{eq}(t)$.

Comparing (3) and (7) we can draw the following conclusions. In the discrete-time case, we want $\|\boldsymbol{\sigma}_{k+1}\|$ to be 0 or small for large k in order for the system's trajectory to reach the switching surface and stay there thereafter. This forces the control law $\boldsymbol{u}_k$ to be $\boldsymbol{u}_{eq,k}$ or within some bound of it. Such a control strategy brings the trajectory of the discrete-time system to the switching surface and keeps it there thereafter. Observe that if $\boldsymbol{u}_k = \boldsymbol{u}_{eq,k}$, then the switching surface is reached in one step. The controller $\boldsymbol{u}_k = \boldsymbol{u}_{eq,k}$ was also analyzed in [14], [1], and [26]. In the continuous-time case the situation is diametrically opposite. If the initial state of the system is not on the switching surface, then in order to reach the surface as fast as possible we should maximize $\|\dot{\boldsymbol{\sigma}}\|$. Applying $\boldsymbol{u}(t) = \boldsymbol{u}_{eq}(t)$ alone in this case would keep the closed-loop system trajectory moving along a surface parallel, but not incidental, to the sliding surface $\boldsymbol{S}\boldsymbol{x} = \boldsymbol{0}$. Therefore, the equivalent control, $\boldsymbol{u}_{eq}(t)$, should not be used in the continuous-time case unless the state is in a desired neighborhood of the switching surface.

Our findings here can be summarized simply as: *One cannot get away from the equivalent control in the discrete-time variable structure control if sliding in the closed-loop system is desired.* In cases where the control law contains a copy of the equivalent control, one should

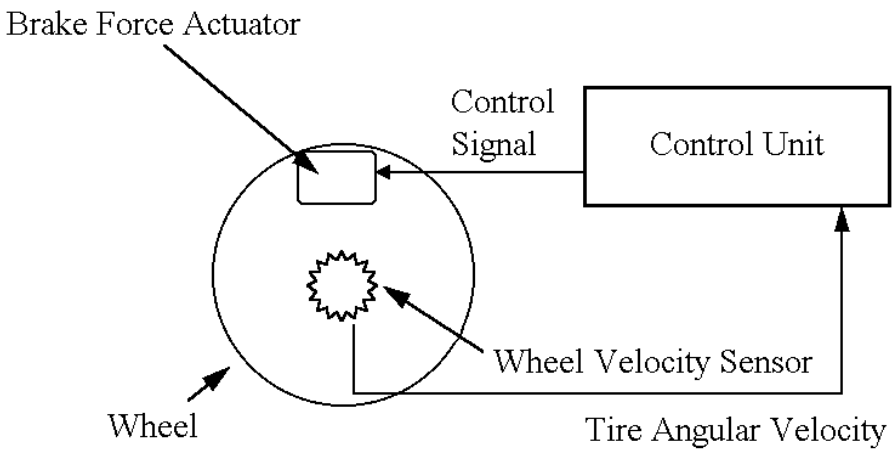

Figure 1: Antilock brake system components.

have a compelling reason for having extra components in the overall control law. If an extra component is used, it should be turned off or made small when the state is in a neighborhood of the switching surface. Furthermore, using the equivalent control alone or equivalent control plus a constant term does not create a variable structure closed-loop system, but rather a linear or an affine system. The perfect sliding mode behavior in discrete-time is achieved with a linear control law.

3 Modeling and Fuzzy Control of Antilock Braking System

The main components of an antilock brake system (ABS) are: a control unit, a brake force actuator, and wheel speed sensors. The controller unit monitors the wheel speed, performs calculations based on the wheel speed, and sends the control signal to the brake force actuator. A diagram of an ABS unit is shown in Figure 1. The ABS system is considered a safety feature in that the main purpose of an ABS is to minimize stopping distance under emergency braking conditions and yet maintain vehicle stability. Antilock brake systems minimize the stopping distance by preventing the wheels from locking up during braking.

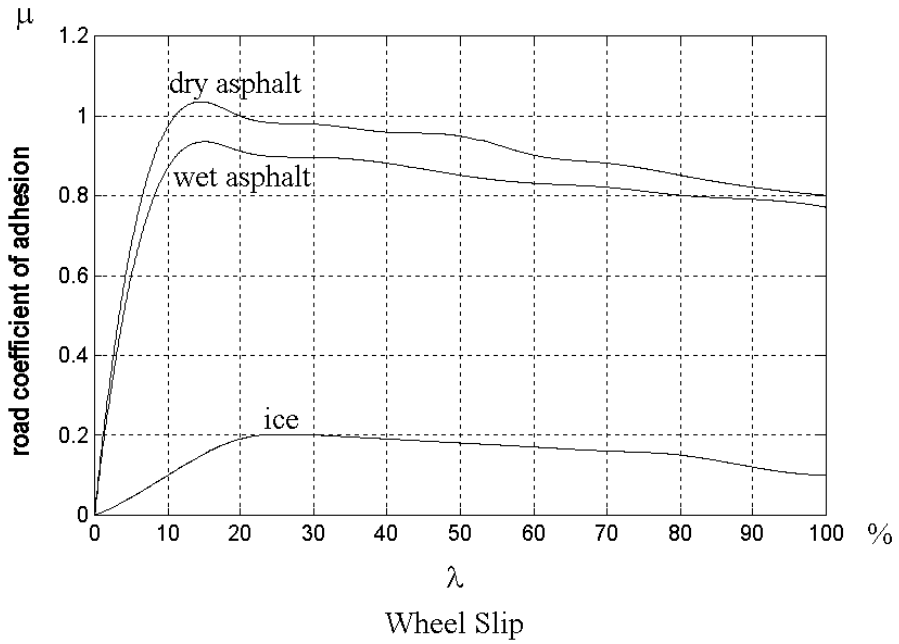

Figure 2: Road coefficient of adhesion versus wheel slip curves for different road surfaces.

The vehicle brake force is proportional to the normal force on the tires. The proportionality factor that relates the vehicle brake force to the tire's normal force is the road coefficient of adhesion. The road coefficient of adhesion is a function of wheel slip as can be seen in Figure 2. The wheel slip is defined as the ratio of the slip velocity in the contact patch (forward velocity minus tire circumferential speed) to forward velocity. Let λ denote the wheel slip, then

$$\lambda = \frac{v - \omega R_w}{v}, \tag{8}$$

where

$$\begin{aligned} v &= \text{vehicle forward velocity} \\ \omega &= \text{tire angular velocity} \\ R_w &= \text{tire rolling radius.} \end{aligned}$$

The above parameters are shown in Figure 3. Note that $0 \leq \lambda \leq 1$. Following the convention,

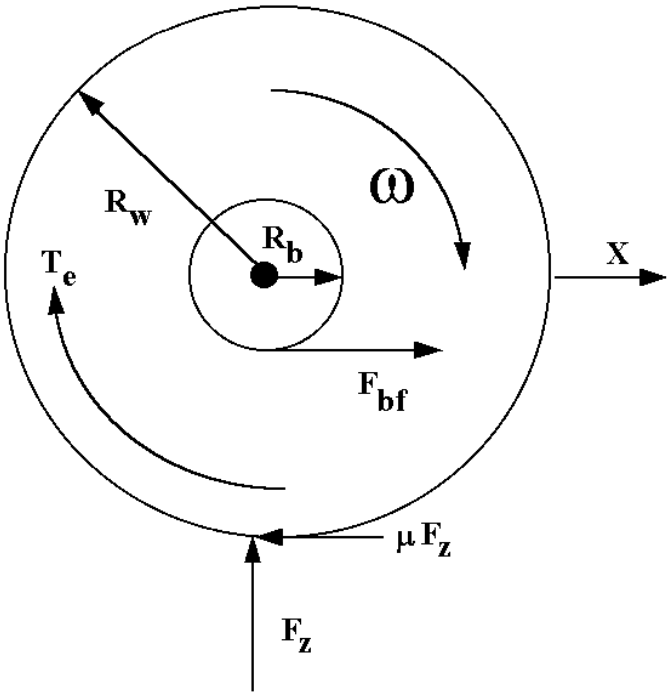

Figure 3: Front wheel free body diagram; for rear wheel F_{bf} becomes F_{br}.

we specify the value of λ using %. Brake lock-up corresponds to 100% wheel slip, and Figure 2 shows that at 100% slip the road coefficient of adhesion is not maximized. The maximum road coefficient of adhesion is attained when the wheels are slipping. Therefore, the maximum braking force acting on the vehicle occurs when the wheels are slipping. Hence, the vehicle stopping distance is minimized by controlling the wheels to slip in the range where the road coefficient of adhesion is maximal. The maximum coefficient of adhesion is in the 5% to 30% slip range. Thus, by allowing the wheels to slip in the 5% to 30% range, we maximize brake force. The operation of an ABS systems is shown in Figure 4 that was adapted from Gillespie [8, page 68]. The application region is the range of slip (point A) where the driver applies the brakes and where the slip level is below impending wheel lock-up. When the wheel slip reaches the range where the coefficient of adhesion is maximized, the ABS system takes control from the driver (point B). The ABS system releases the brake torque before the wheels lock-up (point C) and the wheels begin to pick up speed again. As the wheel speed increases, the wheel slip increases until its slip falls in the maximum brake force region

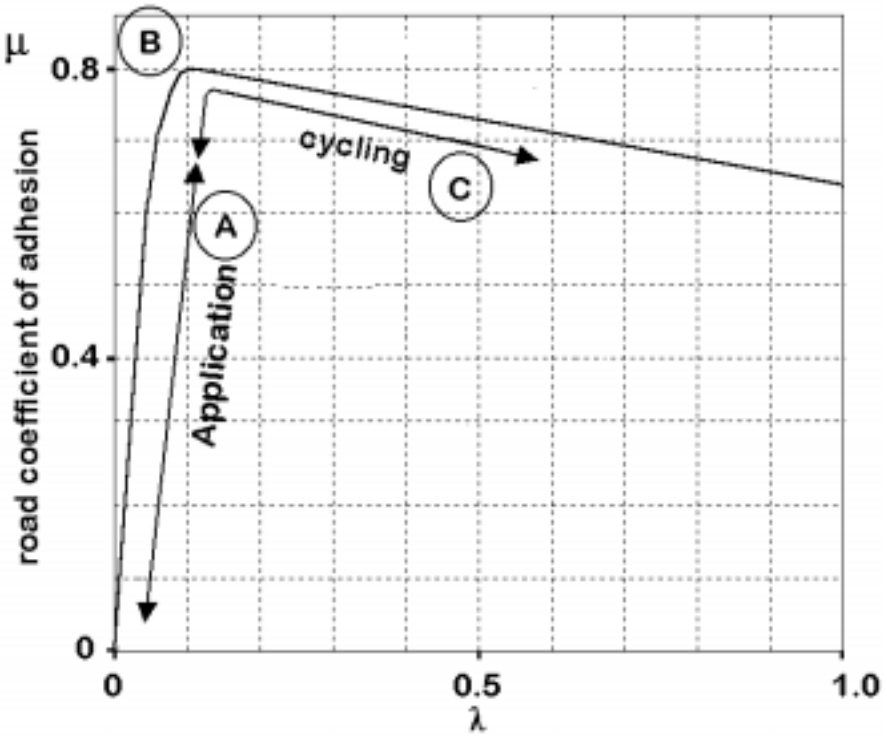

Figure 4: ABS operating modes.

(point B). The ABS system then repeatedly applies the brake torque and releases the brake to keep the wheel slip within the optimal slip region (point B) near the peak of the μ-slip curve.

In our research, we first developed a model for a braking vehicle, and then proposed a fuzzy logic based ABS controller. For a class of analytic nonlinear models that include uncertainties, one can use a sliding mode controller. For instance, Drakunov et al. [3] used a sliding mode approach to develop an ABS controller including a component that performs a search for optimal tire/road friction force. Other sliding mode based ABS controllers were developed by Lin, Dobner, and Fruechte [13] and by us [24]. An alternative approach to the control design for uncertain systems is using fuzzy logic. Mauer [15] developed a fuzzy logic ABS controller using a quarter car model. Layne, Passino, and Yurkovich [11] developed a fuzzy learning ABS controller using a quarter car model. We developed a fuzzy logic ABS controller using our brake system model that includes longitudinal vehicle dynamics, tire dynamics, and a road surface model. This model is non-analytic because we use look-up tables for the road adhesion coefficient. Our results of this research effort were reported in [25].

The brake system we considered by us so far was for straight line braking only. We demonstrated the use of a fuzzy logic controller for an ABS system for a straight line braking on an asphalt surface. However, in our model development we neglected transportation delay caused by the brake hydraulic system and brake pad travel. In our investigation, we found that this transportation delay in the brake system does severely impact the control system's performance. In our future research, we will consider other fuzzy controller designs for brake system models that include transport delay.

As a system enhancement, we believe that using our approach it will be possible to construct a fuzzy controller that also performs a surface identification. When the road surface is identified, the target slip value can be modified according to the surface type. This optimal slip value corresponds to the maximum road coefficient of adhesion for a given surface. Using knowledge of the surface type, the controller should be able to further reduce

stopping distance as compared with the currently available ABS controllers.

4 Fuzzy Adaptive Robust Tracking Controllers

In this section, fuzzy adaptive robust tracking controllers for a class of uncertain dynamical systems are described that was recently developed in our group. Our paper [12] containing the results described below was submitted for publication. The controllers' construction and their analysis involves sliding modes. We have shown that the closed-loop system driven by these controllers is stable and the adaptation parameters are bounded. Simulation results illustrating the performance of the proposed control strategies are included.

4.1 Plant Model and Control Objective

We consider a class of plants modeled by the differential equation

$$x^{(n)} = f(\boldsymbol{x}) + g(\boldsymbol{x})\, u + \eta, \tag{9}$$

where $\boldsymbol{x} = \left[\begin{array}{cccc} x & \dot{x} & \cdots & x^{(n-1)} \end{array} \right]^T$, the functions $f = f(\boldsymbol{x})$ and $g = g(\boldsymbol{x})$ are unknown to us. The function $\eta = \eta(t, \boldsymbol{x})$ models plant's disturbances. We assume that

$$|\eta(t, \boldsymbol{x})| \leq d, \tag{10}$$

where $d > 0$ is known to us. We further assume that the function $g(\boldsymbol{x})$ has a positive lower bound, that is, there exists a positive constant $\underline{g}$ such that $g(\boldsymbol{x}) \geq \underline{g} > 0$. Let

$$\boldsymbol{x}_d = \boldsymbol{x}_d(t) = \left[\begin{array}{cccc} x_d(t) & \dot{x}_d(t) & \cdots & x_d^{(n-1)}(t) \end{array} \right]^T$$

denote the desired state trajectory and let

$$\begin{aligned} \boldsymbol{e} &= \boldsymbol{x} - \boldsymbol{x}_d \\ &= \left[\begin{array}{cccc} x - x_d & \dot{x} - \dot{x}_d & \cdots & x^{(n-1)} - x_d^{(n-1)} \end{array} \right]^T \\ &= \left[\begin{array}{cccc} e & \dot{e} & \cdots & e^{(n-1)} \end{array} \right]^T. \end{aligned}$$

We wish to construct a controller u such that

$$\lim_{t\to\infty} \boldsymbol{e}(t) = \mathbf{0}.$$

We analyze two different fuzzy adaptive tracking controllers and show that the plant (9) driven by these controllers is stable and the adaptation parameters are bounded.

Next, we present background results used by us in the proposed controllers' construction.

4.2 Background Results

4.2.1 Fuzzy Logic System

A fuzzy logic controller with q inputs, $v_1, v_2, \ldots, v_q$, and the center average defuzzifier can be represented as

$$u = \frac{\sum_{l=1}^{m} \prod_{j=1}^{q} \mu_{F_j^l}(v_j)\theta_l}{\sum_{l=1}^{m} \prod_{j=1}^{q} \mu_{F_j^l}(v_j)}, \tag{11}$$

where m is the number of fuzzy rules used to construct the controller, F_j^l is the j-th fuzzy set corresponding to the l-th fuzzy rule, and c_l can be taken as a center of the l-th fuzzy set corresponding to the controller's output, u. To proceed, we represent (11) as

$$u = \sum_{l=1}^{m} \left(\frac{\prod_{j=1}^{q} \mu_{F_j^l}(v_j)}{\sum_{l=1}^{m} \prod_{j=1}^{q} \mu_{F_j^l}(v_j)} \right) \theta_l. \tag{12}$$

Let

$$\boldsymbol{\theta} = \begin{bmatrix} \theta_1 & \theta_2 & \cdots & \theta_m \end{bmatrix}^T$$

and

$$\boldsymbol{\xi} = \begin{bmatrix} \xi_1 & \xi_2 & \cdots & \xi_m \end{bmatrix}^T = \begin{bmatrix} \frac{\prod_{j=1}^{q} \mu_{F_j^1}(v_j)}{\sum_{l=1}^{m} \prod_{j=1}^{q} \mu_{F_j^l}(v_j)} & \cdots & \frac{\prod_{j=1}^{q} \mu_{F_j^m}(v_j)}{\sum_{l=1}^{m} \prod_{j=1}^{q} \mu_{F_j^l}(v_j)} \end{bmatrix}^T.$$

Then, we can represent (12) as

$$u = \boldsymbol{\theta}^T \boldsymbol{\xi}, \tag{13}$$

where the vector $\boldsymbol{\xi}$ is referred to as the *regressor* vector in the control literature.

4.2.2 Projection Operator

Consider a vector-valued function of time,

$$\boldsymbol{\theta}(t) = \begin{bmatrix} \theta_1(t) & \cdots & \theta_m(t) \end{bmatrix}^T \in \mathbb{R}^m,$$

where, $\dot{\theta}_i(t) = \alpha_i(t)$, $i = 1, \cdots, r$. We wish the components $\theta_i(t)$s to lie between $\underline{\theta}_i$ and $\bar{\theta}_i$, that is, $\underline{\theta}_i \leq \theta_i(t) \leq \bar{\theta}_i$. One way to achieve this goal is by setting $\dot{\theta}_i(t) = 0$ when $\theta_i(t)$ reaches either of the bounds and tends to go beyond the bound, that is,

$$\dot{\theta}_i(t) = \begin{cases} 0 & \text{if } \theta_i = \underline{\theta}_i \text{ and } \alpha_i(t) < 0 \\ 0 & \text{if } \theta_i = \bar{\theta}_i \text{ and } \alpha_i(t) > 0 \\ \alpha_i(t) & \text{otherwise.} \end{cases} \tag{14}$$

For compactness, we use the notation *Proj* for the right hand side of (14). Then, we write

$$\dot{\theta}_i(t) = Proj_{\theta_i}(\alpha_i),\ i = 1, \ldots, m, \tag{15}$$

or in vector notation,

$$\dot{\boldsymbol{\theta}}(t) = Proj_{\boldsymbol{\theta}}(\boldsymbol{\alpha}). \tag{16}$$

4.2.3 Sliding Modes

Let

$$\boldsymbol{s} = \begin{bmatrix} s_1 & s_2 & \cdots & s_{n-1} & 1 \end{bmatrix} \in \mathbb{R}^{1\times n}$$

and $\sigma(\boldsymbol{e}) = \boldsymbol{s}\boldsymbol{e}$. Then, $\{\boldsymbol{e} : \sigma(\boldsymbol{e}) = 0\}$ will represent a sliding surface in the tracking error, $\boldsymbol{e}$, space. The coefficients s_i of the sliding surface are chosen in such a way that the system (9) restricted to the sliding surface is asymptotically stable. Our objective is to construct fuzzy tracking controllers that force the tracking error to approach the sliding surface, $\{\sigma(\boldsymbol{e}) = 0\}$, asymptotically and then stay in some neighborhood of the sliding surface for all subsequent time. If f and g were known exactly to us and $\eta = 0$, then the controller

$$u^* = \frac{1}{g}\left(-f - \mu\sigma + x_d^{(n)} - \boldsymbol{k}^T\boldsymbol{e}\right), \tag{17}$$

where

$$\boldsymbol{k} = \begin{bmatrix} 0 & s_1 & \cdots & s_{n-1} \end{bmatrix}^T$$

and $\mu > 0$ is a design parameter, would force the tracking error, e, to behave as desired. We can verify this using standard arguments from sliding mode control practice—see, for example, [2]. We consider the function $V = \frac{1}{2}\sigma^2$. Note that V is positive definite with respect to the sliding surface $\{\sigma = 0\}$. The function V can be viewed as a distance measure to the sliding surface $\{\sigma = 0\}$. The time derivative of V evaluated on the trajectories of the closed-loop system (9), (17) is

$$\begin{aligned} \dot{V} &= \sigma\dot{\sigma} \\ &= \sigma \boldsymbol{s} \frac{d\boldsymbol{e}}{dt} \\ &= \sigma\left(e^{(n)} + s_{n-1}e^{(n-1)} + \cdots + s_1\dot{e}\right) \\ &= \sigma\left(x^{(n)} - x_d^{(n)} + \boldsymbol{k}^T\boldsymbol{e}\right) \\ &= \sigma\left(f + gu - x_d^{(n)} + \boldsymbol{k}^T\boldsymbol{e}\right) \end{aligned} \tag{18}$$

Substituting into the above equation the control law given by (17) gives

$$\dot{V} = -\mu\sigma^2. \tag{19}$$

Thus, the sliding surface, $\{\sigma = 0\}$, is asymptotically attractive and the system restricted to the sliding surface can be made asymptotically stable with respect to the origin by an appropriate choice of the parameters, s_i, of the sliding surface.

The control law (17) requires perfect knowledge of the plant's model. However, the plant model components f and g are unknown to us. We next describe how to use adaptive fuzzy logic controllers to approximate, as closely as possible, the performance of (17). In what follows, we consider two cases. The first case is when the function $f = f(\boldsymbol{x})$ is unknown to us while $g = g(\boldsymbol{x}) > 0$ is known to us. The second case is when both f and g are unknown to us. In both cases, we consider the presence of a bounded disturbance modeled by η.

4.3 The Controllers

4.3.1 Unknown $f(\boldsymbol{x})$

When in our plant model (9) only $g(\boldsymbol{x})$ is known, $\eta \neq 0$, and $f(\boldsymbol{x})$ is unknown, we propose to approximate $f(\boldsymbol{x})$ with fuzzy logic system of the form $\boldsymbol{\theta}_f^T \boldsymbol{\xi}_f(\boldsymbol{x})$, where the functions $\boldsymbol{\theta}_f$ and $\boldsymbol{\xi}_f$ will be described after defining relevant symbols. We denote by $\boldsymbol{\theta}_f^*$ an "optimal" vector such that

$$\boldsymbol{\theta}_f^* = \text{argmin}_{\boldsymbol{\theta}_f} \sup_{\boldsymbol{x} \in \Omega} \left| f(\boldsymbol{x}) - \boldsymbol{\theta}_f^T \boldsymbol{\xi}_f(\boldsymbol{x}) \right|, \tag{20}$$

where $\Omega \subseteq \mathbb{R}^n$ is a region to which the state $\boldsymbol{x}$ is constrained to reside. We assume that

$$\left| f(\boldsymbol{x}) - \boldsymbol{\theta}_f^{*T} \boldsymbol{\xi}_f(\boldsymbol{x}) \right| \leq d_f, \quad \forall\, \boldsymbol{x} \in \Omega, \tag{21}$$

where $d_f > 0$ and each element of $\boldsymbol{\theta}_f^*$ is a constant and bounded below and above as follows

$$\underline{\theta}_{fi} \leq \theta_{fi}^* \leq \bar{\theta}_{fi}, \quad \text{for all } i = 1, \ldots, r, \tag{22}$$

or in vector notation,

$$\underline{\boldsymbol{\theta}}_f \leq \boldsymbol{\theta}_f^* \leq \bar{\boldsymbol{\theta}}_f. \tag{23}$$

We define the adaptation parameter error as

$$\boldsymbol{\phi}_f = \boldsymbol{\theta}_f - \boldsymbol{\theta}_f^*. \tag{24}$$

We use the adaptation law

$$\dot{\boldsymbol{\phi}}_{\boldsymbol{f}}(t) = \dot{\boldsymbol{\theta}}_f(t) = Proj_{\boldsymbol{\theta}_f}(\gamma_f \sigma \boldsymbol{\xi}_f(t)), \tag{25}$$

where $\gamma_f > 0$ is a design parameter. It is easy to verify, using the definition of $Proj$ and the fact that $\underline{\theta}_{fi} \leq \theta_{fi}^* \leq \bar{\theta}_{fi}$ for each i, that

$$\boldsymbol{\phi}_f^T \left(\frac{1}{\gamma_f} Proj_{\boldsymbol{\theta}_f} \left(\gamma_f \sigma \boldsymbol{\xi}_f \right) - \sigma \boldsymbol{\xi}_f \right) \leq 0. \tag{26}$$

We propose the following fuzzy adaptive control law,

$$\boxed{u = \frac{1}{g} \left(-\boldsymbol{\theta}_f^T \boldsymbol{\xi}_f - \mu\sigma + x_d^{(n)} - \boldsymbol{k}^T \boldsymbol{e} + u_s \right)} \tag{27}$$

with u_s satisfying

$$\sigma\left(f - \boldsymbol{\theta}_f^T \boldsymbol{\xi}_f + u_s + \eta\right) \leq \epsilon, \tag{28}$$

$$\sigma u_s \leq 0, \tag{29}$$

where $\epsilon > 0$ is a design parameter. We now state a theorem concerning the dynamical behavior of the closed-loop system driven by the control law (27). A proof of the theorem can be found in [12].

Theorem 1 *For the closed-loop system,*

$$\left.\begin{array}{rcl} x^{(n)} & = & f + gu + \eta \\ u & = & \frac{1}{g}\left(-\boldsymbol{\theta}_f^T \boldsymbol{\xi}_f - \mu\sigma + x_d^{(n)} - \boldsymbol{k}^T \boldsymbol{e} + u_s\right) \\ \dot{\boldsymbol{\theta}}_f & = & Proj_{\boldsymbol{\theta}_f}(\gamma_f \sigma \boldsymbol{\xi}_f) \end{array}\right\} \tag{30}$$

where u_s satisfies (28) and (29), we have:

(i)

$$\sigma^2(t) \leq e^{-2\mu t}\sigma^2(0) + \frac{\epsilon}{\mu}; \tag{31}$$

(ii) if $\eta = 0$ and there exists $\boldsymbol{\theta}_f^*$ such that $f(\boldsymbol{x}) = \boldsymbol{\theta}_f^{*T} \boldsymbol{\xi}_f(\boldsymbol{x})$, then the origin of the $(\sigma,\ \boldsymbol{\phi}_f)$-space is stable, and hence $\sigma(t)$ and $\boldsymbol{\phi}_f(t)$ are bounded for all $t \geq 0$ and $e(t) \to 0$ as $t \to \infty$.

4.3.2 Selecting u_s in control law (27)

We now discuss a method that can be used to select the component u_s while implementing the control law (27)). Let h be a constant such that

$$h \geq \left\|\boldsymbol{\xi}_f\right\| \left\|\bar{\boldsymbol{\theta}}_f - \underline{\boldsymbol{\theta}}_f\right\|.$$

Given the design parameter ϵ, choose positive numbers ϵ_1, ϵ_2, and ϵ_3 such that $\epsilon = \epsilon_1 + \epsilon_2 + \epsilon_3$. Then, u_s can be chosen as

$$u_s = -k_s \sigma, \tag{32}$$

where

$$k_s \geq \frac{d_f^2}{4\epsilon_1} + \frac{h^2}{4\epsilon_2} + \frac{d^2}{4\epsilon_3}. \tag{33}$$

We verify that the above choice of u_s guarantees that (32) satisfies (28) and (29). We first consider the left-hand side of (28). Adding and subtracting $\boldsymbol{\theta}_f^{*T}\boldsymbol{\xi}_f$ and using (24) yields

$$\begin{aligned}\sigma(f - \boldsymbol{\theta}_f^T\boldsymbol{\xi}_f + u_s + \eta) &= \sigma(f - \boldsymbol{\theta}_f^{*T}\boldsymbol{\xi}_f + \boldsymbol{\theta}_f^{*T}\boldsymbol{\xi}_f - \boldsymbol{\theta}_f^T\boldsymbol{\xi}_f + u_s + \eta) \\ &= \sigma(f - \boldsymbol{\theta}_f^{*T}\boldsymbol{\xi}_f - \boldsymbol{\phi}_f{}^T\boldsymbol{\xi}_f - k_s\sigma + \eta). \end{aligned} \tag{34}$$

We now use (33) and group the terms to obtain

$$\begin{aligned}\sigma(f - \boldsymbol{\theta}_f^T\boldsymbol{\xi}_f + u_s + \eta) \leq\ & \sigma\left(f - \boldsymbol{\theta}_f^{*T}\boldsymbol{\xi}_f - \frac{d_f^2}{4\epsilon_1}\sigma\right) \\ & -\sigma\left(\boldsymbol{\phi}_f{}^T\boldsymbol{\xi}_f + \frac{h^2}{4\epsilon_2}\sigma\right) + \sigma\left(\eta - \frac{d^2}{4\epsilon_3}\sigma\right). \end{aligned} \tag{35}$$

Next, we consider each term on the right hand side of the above inequality separately. We start with the first term. Completing the squares, we obtain

$$\sigma\left(f - \boldsymbol{\theta}_f^{*T}\boldsymbol{\xi}_f - \frac{d_f^2}{4\epsilon_1}\sigma\right) = -\left(\frac{d_f}{2\sqrt{\epsilon_1}}\sigma - \frac{f - \boldsymbol{\theta}_f^{*T}\boldsymbol{\xi}_f}{d_f/\sqrt{\epsilon_1}}\right)^2 + \left(\frac{f - \boldsymbol{\theta}_f^{*T}\boldsymbol{\xi}_f}{d_f/\sqrt{\epsilon_1}}\right)^2.$$

Neglecting the first term in the above and using the assumption (21), we get

$$\sigma\left(f - \boldsymbol{\theta}_f^{*T}\boldsymbol{\xi}_f - \frac{d_f^2}{4\epsilon_1}\sigma\right) \leq \frac{d_f^2}{d_f^2/\epsilon_1} \leq \epsilon_1. \tag{36}$$

Completing the squares in the second term on the right-hand side of (35) gives

$$\begin{aligned} -\sigma\left(\boldsymbol{\phi}_f{}^T\boldsymbol{\xi}_f + \frac{h^2}{4\epsilon_2}\sigma\right) &= -\left(\frac{h}{2\sqrt{\epsilon_2}}\sigma + \frac{\boldsymbol{\phi}_f^T\boldsymbol{\xi}_f}{h/\sqrt{\epsilon_2}}\right)^2 + \left(\frac{\boldsymbol{\phi}_f^T\boldsymbol{\xi}_f}{h/\sqrt{\epsilon_2}}\right)^2 \\ &\leq \left(\frac{\boldsymbol{\phi}_f^T\boldsymbol{\xi}_f}{h/\sqrt{\epsilon_2}}\right)^2 \\ &= \left(\frac{(\boldsymbol{\theta}_f - \boldsymbol{\theta}_f^*)^T\boldsymbol{\xi}}{h}\right)^2 \epsilon_2 \\ &\leq \frac{\left\|\boldsymbol{\theta}_f - \boldsymbol{\theta}_f^*\right\|^2 \left\|\boldsymbol{\xi}_f\right\|^2}{h^2}\epsilon_2 \\ &\leq \frac{\left\|\boldsymbol{\theta}_f - \boldsymbol{\theta}_f^*\right\|^2 \left\|\boldsymbol{\xi}_f\right\|^2}{\left\|\boldsymbol{\xi}_f\right\|^2 \left\|\bar{\boldsymbol{\theta}}_f - \underline{\boldsymbol{\theta}}_f\right\|^2}\epsilon_2 \qquad (37) \\ &\leq \epsilon_2. \qquad (38) \end{aligned}$$

Completing the squares in the third term on the right-hand side of (35) yields

$$\begin{aligned}\sigma\left(\eta(t)-\frac{d^2}{4\epsilon_3}\sigma\right) &= -\left(\frac{d}{2\sqrt{\epsilon_3}}\sigma-\frac{\eta}{d/\sqrt{\epsilon_3}}\right)^2+\frac{\eta^2}{d^2}\epsilon_3\\ &\leq \epsilon_3.\end{aligned}$$

Thus,

$$\sigma\left(f-\boldsymbol{\theta}_f^T\boldsymbol{\xi}_f+u_s+\eta\right)\leq\epsilon_1+\epsilon_2+\epsilon_3=\epsilon.$$

and hence (28) is satisfied.

Also, $u_s=-k_s\sigma$, $k_s>0$, satisfies (29).

4.3.3 Unknown $f(\boldsymbol{x})$ and $g(\boldsymbol{x})$

Assume now that $g(\boldsymbol{x})$ and $f(\boldsymbol{x})$ are unknown to us and $\eta\neq 0$. We approximate $f(\boldsymbol{x})$ and $g(\boldsymbol{x})$ with fuzzy logic systems, $\boldsymbol{\theta}_f^T\boldsymbol{\xi}_f(\boldsymbol{x})$ and $\boldsymbol{\theta}_g^T\boldsymbol{\xi}_g(\boldsymbol{x})$, respectively. The conditions on $\boldsymbol{\theta}_f^T\boldsymbol{\xi}_f(\boldsymbol{x})$ are the same as in the previous case, and the conditions on $\boldsymbol{\theta}_g^T\boldsymbol{\xi}_g(\boldsymbol{x})$ are similar, that is, the optimal parameter vector, $\boldsymbol{\theta}_g^*$, is

$$\boldsymbol{\theta}_g^*=\text{argmin}_{\boldsymbol{\theta}_g}\sup_{\boldsymbol{x}\in\Omega}\left|g(\boldsymbol{x})-{\boldsymbol{\theta}_g}^T\boldsymbol{\xi}_g(\boldsymbol{x})\right|. \tag{39}$$

We assume that

$$\left|g(\boldsymbol{x})-{\boldsymbol{\theta}_g^*}^T\boldsymbol{\xi}(\boldsymbol{x})\right|\leq d_g,\quad \text{for all } \boldsymbol{x}\in\Omega, \tag{40}$$

where

$$\underline{\theta}_{gi}\leq\theta_{gi}^*\leq\bar{\theta}_{gi},\quad \text{for all } i=1,\cdots,r. \tag{41}$$

The parameter error, $\boldsymbol{\phi}_g=\boldsymbol{\theta}_g-\boldsymbol{\theta}_g^*$, is adapted according to the law,

$$\dot{\boldsymbol{\phi}}_{\boldsymbol{g}}=\dot{\boldsymbol{\theta}}_g=Proj_{\boldsymbol{\theta}_g}(\gamma_g\sigma\boldsymbol{\xi}_g u_a),$$

where

$$u_a=\frac{1}{\boldsymbol{\theta}_g^T\boldsymbol{\xi}_g}\left(-\boldsymbol{\theta}_f^T\boldsymbol{\xi}_f+x_d^{(n)}-\boldsymbol{k}^T\boldsymbol{e}\right). \tag{42}$$

The initial values of the components of $\boldsymbol{\theta}_g$ are chosen to satisfy (41), where for each $i=1,\ldots,r$, we have $\theta_{gi}>0$. This ensures that $\boldsymbol{\theta}_g^T\boldsymbol{\xi}_g>0$ because we choose fuzzy sets so that

at any t at least one rule fires and so at least one component of $\boldsymbol{\xi}$ is nonzero and in fact positive. Using the definition of $Proj$, one can verify that

$$\boldsymbol{\phi}_g^T \left(\frac{1}{\gamma_g} Proj_{\boldsymbol{\theta}_g} \left(\gamma_g \sigma \boldsymbol{\xi}_g u_a \right) - \sigma \boldsymbol{\xi}_g u_a \right) \leq 0. \tag{43}$$

We propose the following fuzzy adaptive control law,

$$\boxed{u = \frac{1}{\boldsymbol{\theta}_g^T \boldsymbol{\xi}_g} \left(-\boldsymbol{\theta}_f^T \boldsymbol{\xi}_f + x_d^{(n)} - \boldsymbol{k}^T \boldsymbol{e} \right) - \frac{1}{\underline{g}} \mu \sigma + u_s} \tag{44}$$

with u_s satisfying the following conditions,

$$\sigma \left(f - x_d^{(n)} + \boldsymbol{k}^T \boldsymbol{e} + g u_a + g u_s + \eta \right) \leq \epsilon, \tag{45}$$

$$\sigma u_s \leq 0, \tag{46}$$

where $\epsilon > 0$ is a design parameter. Using the definition of u_a, given by (42), we represent (44) as

$$u = u_a - \frac{1}{\underline{g}} \mu \sigma + u_s. \tag{47}$$

Our findings are summarized in the following theorem, whose proof can be found in [12].

Theorem 2 *For the closed-loop system,*

$$\left.\begin{array}{rcl} x^{(n)} & = & f + gu + \eta \\ u & = & \frac{1}{\boldsymbol{\theta}_g^T \boldsymbol{\xi}_g} \left(-\boldsymbol{\theta}_f^T \boldsymbol{\xi}_f + x_d^{(n)} - \boldsymbol{k}^T \boldsymbol{e} \right) - \frac{1}{\underline{g}} \mu \sigma + u_s \\ \dot{\boldsymbol{\theta}}_f & = & Proj_{\boldsymbol{\theta}_f} (\gamma_f \sigma \boldsymbol{\xi}_f) \\ \dot{\boldsymbol{\theta}}_g & = & Proj_{\boldsymbol{\theta}_g} (\gamma_g \sigma \boldsymbol{\xi}_g u_a) \end{array}\right\} \tag{48}$$

where u_s satisfies (45) and (46), we have:

(i)

$$\sigma^2(t) \leq e^{-2\mu t} \sigma^2(0) + \frac{\epsilon}{\mu}; \tag{49}$$

(ii) if $\eta = 0$ and there exist $\boldsymbol{\theta}_f^*$ and $\boldsymbol{\theta}_g^*$ such that $f(\boldsymbol{x}) = \boldsymbol{\theta}_f^{*T} \boldsymbol{\xi}_f(\boldsymbol{x})$ and $g(\boldsymbol{x}) = \boldsymbol{\theta}_g^{*T} \boldsymbol{\xi}_g(\boldsymbol{x})$, then the origin of the $\left[\begin{array}{ccc} \sigma & \boldsymbol{\phi}_f & \boldsymbol{\phi}_g \end{array} \right]^T$-space is stable and hence $\sigma(t)$, $\boldsymbol{\phi}_f(t)$, and $\boldsymbol{\phi}_g(t)$ are bounded and $e(t) \to 0$ as $t \to \infty$.

4.3.4 Selecting u_s in control law (44)

The component u_s appearing in the control law (44) can be chosen similarly as in the previous case. We need a lower bound on the gain k_s. Let

$$h_f \geq \left\|\boldsymbol{\xi}_f\right\| \left\|\bar{\boldsymbol{\theta}}_f - \underline{\boldsymbol{\theta}}_f\right\| \text{ and } h_g \geq \left\|\boldsymbol{\xi}_g\right\| \left\|\bar{\boldsymbol{\theta}}_g - \underline{\boldsymbol{\theta}}_g\right\| |u_a| \,.$$

Given the design parameter ϵ, select positive numbers $\epsilon_1,\ \epsilon_2,\ \epsilon_3$, and ϵ_4 such that $\epsilon = \epsilon_1 + \epsilon_2 + \epsilon_3 + \epsilon_4$. Then, k_s should satisfy the following condition,

$$k_s \geq \frac{1}{\underline{g}} \left(\frac{d_f^2 + u_a^2 d_g^2}{2\epsilon_1} + \frac{h_f^2}{4\epsilon_2} + \frac{h_g^2}{4\epsilon_3} + \frac{d^2}{4\epsilon_4} \right). \tag{50}$$

When the gain k_s satisfies the above condition, $u_s = -k_s\sigma$ guarantees that (45) and (46) are satisfied. To show that this is indeed the case, consider the left-hand side of (45). Use $\boldsymbol{\theta}_g^T \boldsymbol{\xi}_g u_a + \boldsymbol{\theta}_f^T \boldsymbol{\xi}_f = x_d^{(n)} - \boldsymbol{k}^T \boldsymbol{e}$ from (42), and then add and subtract $\boldsymbol{\theta}_f^{*T} \boldsymbol{\xi}_f$ and $\boldsymbol{\theta}_g^{*T} \boldsymbol{\xi}_g u_a$ to obtain

$$\begin{aligned} \sigma\left(f - x_d^{(n)} + \boldsymbol{k}^T \boldsymbol{e} + g u_a + g u_s + \eta\right) &= \sigma\left(f - \boldsymbol{\theta}_f^T \boldsymbol{\xi}_f - \boldsymbol{\theta}_g^T \boldsymbol{\xi}_g u_a + g u_a + g u_s + \eta\right) \\ &= \sigma\Big(f - \boldsymbol{\theta}_f^{*T} \boldsymbol{\xi}_f - \boldsymbol{\phi}_f^T \boldsymbol{\xi}_f + (g - \boldsymbol{\theta}_g^{*T} \boldsymbol{\xi}_g) u_a \\ &\qquad - \boldsymbol{\phi}_g^T \boldsymbol{\xi}_g u_a + g u_s + \eta\Big) \,. \end{aligned}$$

Taking into account (50) in the above and rearranging terms gives

$$\begin{aligned} \sigma\left(f - x_d^{(n)} + \boldsymbol{k}^T e + g u_a + g u_s + \eta\right) \leq\ & \sigma\left(f - \boldsymbol{\theta}_f^T \boldsymbol{\xi}_f - \frac{d_f^2}{2\epsilon_1}\sigma\right) \\ & + \sigma\left(\left(g - \boldsymbol{\theta}_g^{*T} \boldsymbol{\xi}_g\right) u_a - \frac{u_a^2 d_g^2}{2\epsilon_1}\sigma\right) \\ & - \sigma\left(\boldsymbol{\phi}_f^T \boldsymbol{\xi}_f + \frac{h_f^2}{4\epsilon_2}\sigma\right) - \sigma\left(\boldsymbol{\phi}_g^T \boldsymbol{\xi}_g u_a + \frac{h_g^2}{4\epsilon_3}\sigma\right) \\ & + \sigma\left(\eta - \frac{d^2}{4\epsilon_4}\sigma\right). \end{aligned}$$

Completing the squares, similarly as in the previous case, yields

$$\sigma\left(f - x_d^{(n)} + \boldsymbol{k}^T e + g u_a + g u_s + \eta\right) \leq \left(\frac{f - \boldsymbol{\theta}_f^T \boldsymbol{\xi}_f}{\sqrt{2} d_f / \sqrt{\epsilon_1}}\right)^2 + \left(\frac{(g - \boldsymbol{\theta}_g^{*T} \boldsymbol{\xi}_g) u_a}{\sqrt{2}\,|u_a|\, d_g / \sqrt{\epsilon_1}}\right)^2$$

$$
\begin{aligned}
&+\left(\frac{\boldsymbol{\phi}_f^T\boldsymbol{\xi}_f}{h_f^2/\sqrt{\epsilon_2}}\right)^2+\left(\frac{\boldsymbol{\phi}_g^T\boldsymbol{\xi}_g u_a}{h_g^2/\sqrt{\epsilon_3}}\right)^2+\left(\frac{\eta}{d/\sqrt{\epsilon_4}}\right)^2\\
\leq\ & \frac{1}{2}\epsilon_1+\frac{1}{2}\epsilon_1+\epsilon_2+\epsilon_3+\epsilon_4\\
=\ & \epsilon.
\end{aligned}
$$

Hence, (45) is satisfied, and so is (46) by the fact that $u_s = -k_s\sigma$, where $k_s > 0$.

4.4 Examples

In this Subsection, we present simulation results illustrating the performance of the proposed control strategies. The controllers are tested on a simplified model of an electric drive system used by Fischle and Schröder [4] to test their fuzzy adaptive controllers. The plant is modeled by the differential equation,

$$\ddot{x} = -\frac{5}{J}\arctan(5\dot{x}) + \frac{c_T}{J}u = f(x,\dot{x}) + gu, \tag{51}$$

where x is the angular position, c_T =10 Nm/A, and J = 0.1 kg·m^2. The reference signal x_d is generated by the reference system whose transfer function is given by $\frac{400}{s^2+40s+400}$. The input signal, $w(t)$, to the reference system is changing its value randomly between -1.5 and 1.5 every 0.5 seconds.

Example 1 In this example, we assume that we know g, where $g = 100$, and that there are no disturbances affecting the system, that is, $\eta = 0$. We use the control law given by (27), where $f(\boldsymbol{x})$ is approximated by a fuzzy logic system. We use fuzzy sets for x and $\dot{x}$ as in Fischle and Schröder [4]. They are shown in Figure 5. There are two fuzzy sets for x and six fuzzy sets for $\dot{x}$. Thus, we can have twelve fuzzy rules possible. They have the form:

Rule 1: IF x is N AND $\dot{x}$ is LN THEN $y = \theta_1$

$\vdots$

Rule 12: IF x is P AND $\dot{x}$ is LP THEN $y = \theta_{12}$,

where θ_i, $i = 1,\ldots,12$ are the adaptation parameters. The bounds on the components of the adaptation parameter vector, $\boldsymbol{\theta}_f$, are chosen as $\bar{\theta}_f = 200$ and $\underline{\theta}_f = -200$. All the

initial values of the components of $\boldsymbol{\theta}_f$ are set to zero. If we had expert knowledge about the plant operation, we could incorporate this information into the controller design by selecting appropriately the initial values of the adaptation parameters. We choose $d_f = 50$ and $d_g = 10$, and $\gamma_f = 5000$. The remaining design parameters are: $\mu = 250$, $\epsilon_1 = 50$, $\epsilon_2 = 50$. As $\eta(t) = 0$, we do not need to worry about ϵ_3.

We used SIMULINK to simulate the dynamical behavior of the closed-loop system. Its block diagram is depicted in Figure 6. The regressor generator block produces ξ from the input x and the parameter adaptation block updates $\boldsymbol{\theta}_f$. It is made up of sets of integrators as shown in Figure 7. The $\boldsymbol{s}$ vector that defines the sliding surface, $\{\boldsymbol{e} : \boldsymbol{s}\boldsymbol{e} = 0\}$, was chosen as $\boldsymbol{s} = \begin{bmatrix} 40 & 1 \end{bmatrix}$. The simulation results are shown in Figures 8 and 9. The output $x(t)$, the reference signal $x_d(t)$, and the tracking error $e(t)$ are shown in Figure 8. The tracking error, $e(t)$, is so small that one cannot distinguish between the actual state $x(t)$ and the desired state $x_d(t)$. The plots of the control signal u and the components of $\boldsymbol{\theta}_f$ versus time are depicted in Figure 9. As the fuzzy logic system adapts the parameter $\boldsymbol{\theta}_f$, the error, $e(t)$, gets smaller and smaller. If we used smaller ϵ, then we would achieve even smaller tracking error at the expense of higher control effort.

Example 2 In this example, it is assumed that $f(\boldsymbol{x})$ and g are unknown to us and the control law (44) is employed. Unknown $f(\boldsymbol{x})$ and g are approximated by two separate fuzzy logic systems using fuzzy sets shown in Figure 5 for both fuzzy logic systems.

The bounds on the adaptation parameters are chosen as: $\bar{\theta}_f = 200$, $\underline{\theta}_f = -200$, $\bar{\theta}_g = 150$, and $\underline{\theta}_g = 50$. All the initial values of the components of the adaptation parameter vector $\boldsymbol{\theta}_f$ are set to zero. The initial values of $\boldsymbol{\theta}_g$ are set to 150 to avoid excessively large control signal in the early stages of the simulation run. The selected gains are $\gamma_f = 5000$ and $\gamma_g = 1000$. The other design parameters are: $\epsilon_1 = 50$, $\epsilon_2 = 100$, $\epsilon_3 = 50$, and $\epsilon_4 = 50$. The remaining parameters are the same as in the previous example.

SIMULINK block diagrams of the closed-loop system and the parameter adaptation law are depicted in Figure 10 and Figure 14, respectively. The disturbance, η, is a random signal, whose plot versus time is shown in Figure 13. We used $d = 100$ so that the condition,

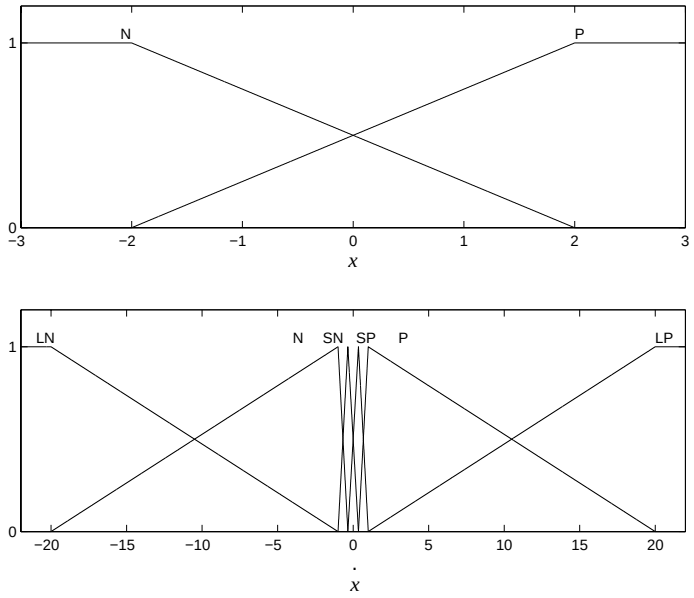

Figure 5: Fuzzy sets for x and $\dot{x}$.

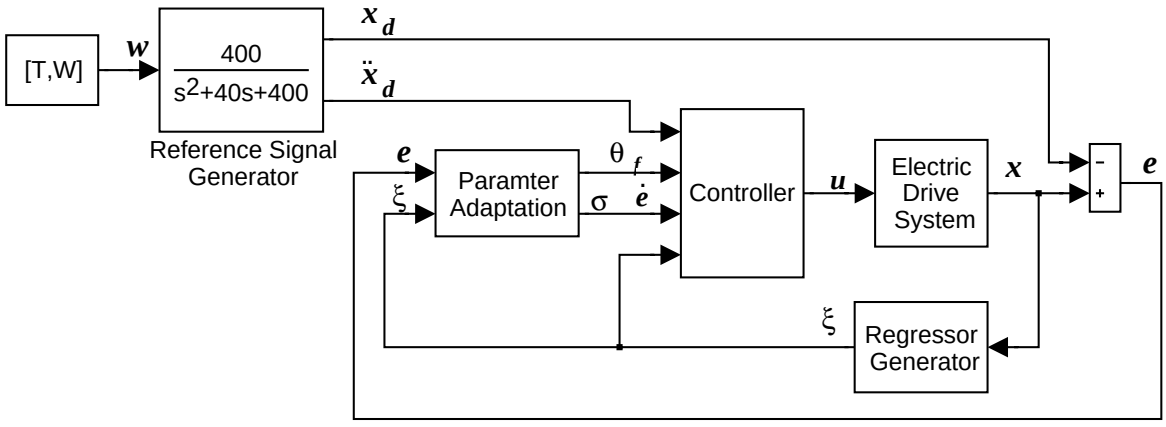

Figure 6: SIMULINK block diagram of fuzzy adaptive robust control system of Example 1.

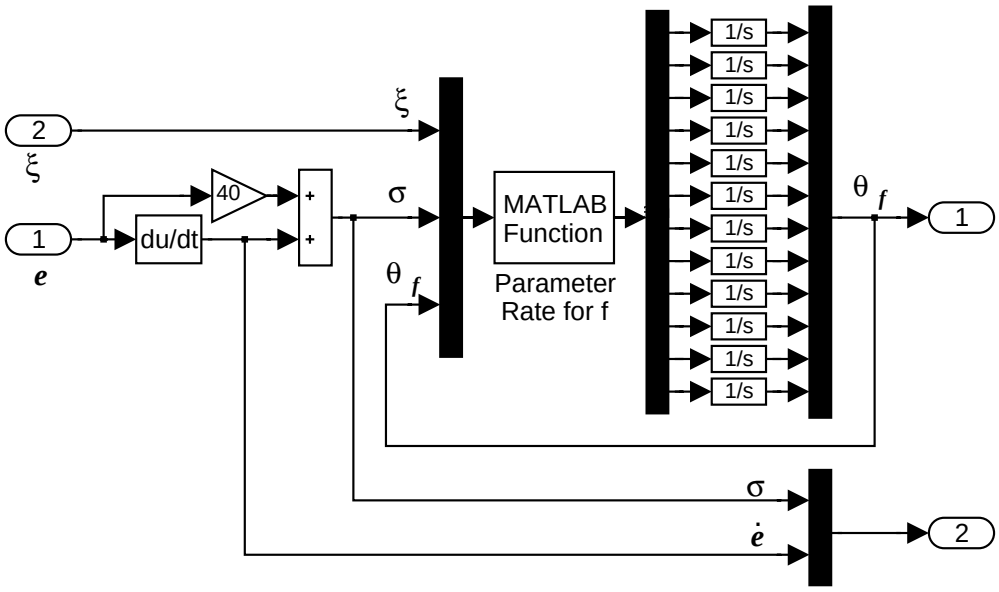

Figure 7: Parameter adaptation block of Example 1.

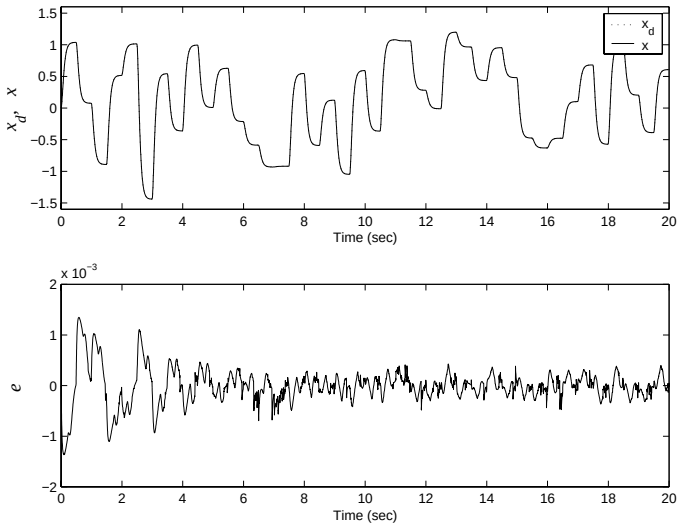

Figure 8: Plots of $x(t)$ and error $e(t)$ in Example 1.

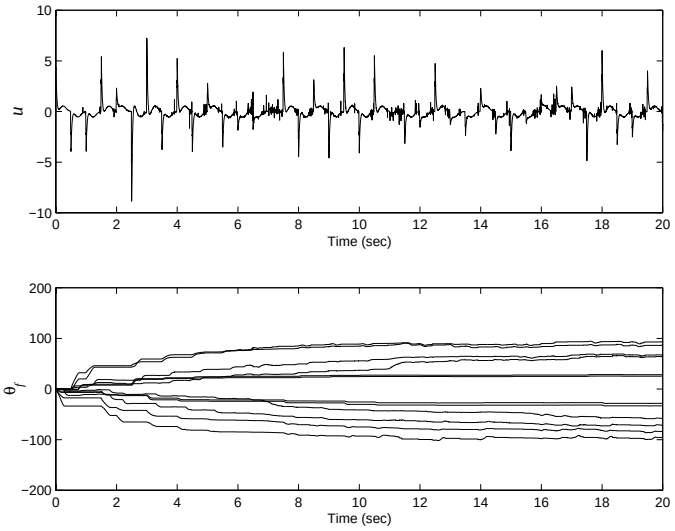

Figure 9: Plots of control effort $u(t)$ and the components of the parameter vector $\boldsymbol{\theta}_f$ versus time in Example 1.

$|\eta(t)| \leq d$, is satisfied. We chose, as before, $\boldsymbol{s} = \begin{bmatrix} 40 & 1 \end{bmatrix}$. The simulation results are shown in Figures 12, 13, and 14. As can be seen in Figure 12, the tracking error, $e(t)$, remains very small even in the presence of the disturbance, η. Plots of the time history of the adaptation parameters are shown in Figure 14.

5 Presentations

The research progress is monitored through weekly meetings of the principal investigator and Ph.D. students working on the project to discuss accomplishments and difficulties. During these meetings the students present the results obtained by them or others to their peers. Yonggon Lee who is one of the Ph.D. students working on the project, has been chosen a third place student presenter at the Spring 2000 Workshop of the Electrical and Computer Engineering Industrial Affiliates Workshop. Our group is in process of preparing papers to be submitted to the next American Control Conference (ACC) as well as to the next Conference on Decision and Control (CDC).

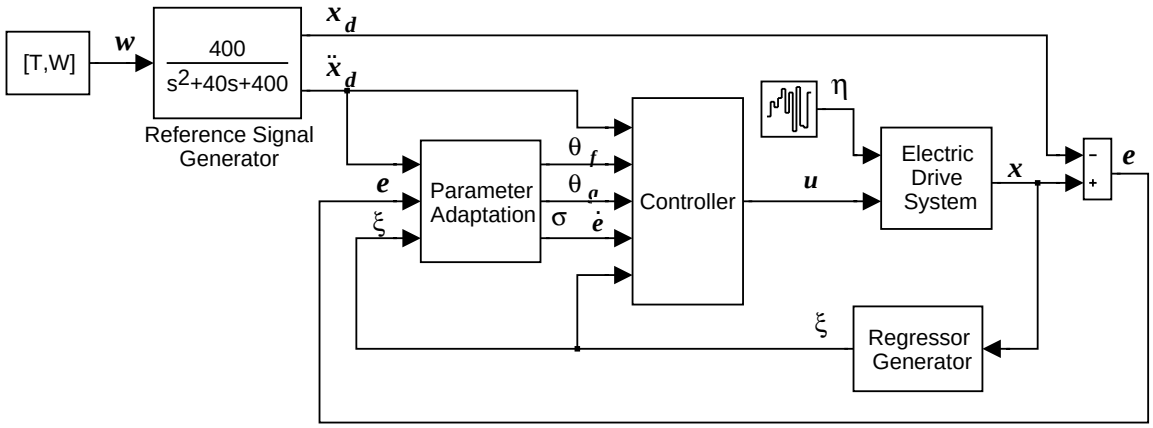

Figure 10: SIMULINK block diagram of the fuzzy adaptive robust control system of Example 2.

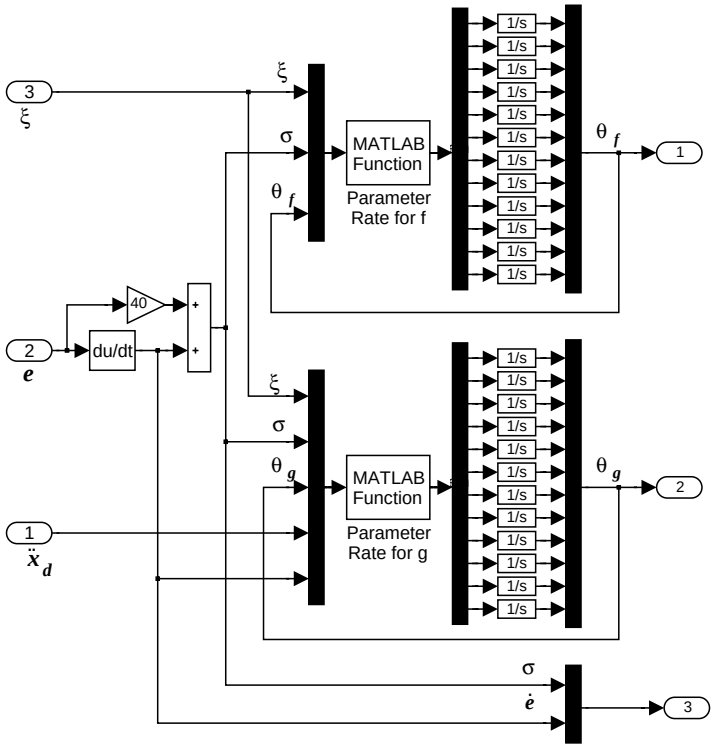

Figure 11: Parameter adaptation block of Example 2.

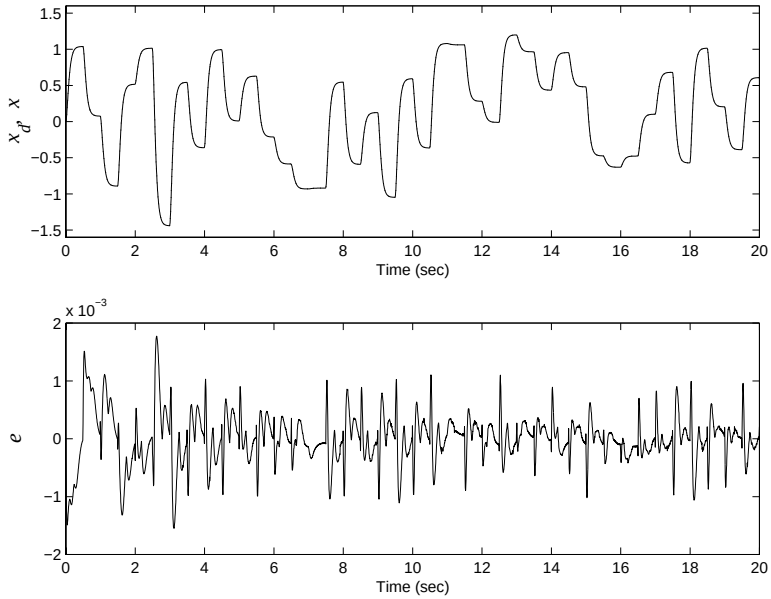

Figure 12: Plots of $x(t)$ and error $e(t)$ versus time in Example 2.

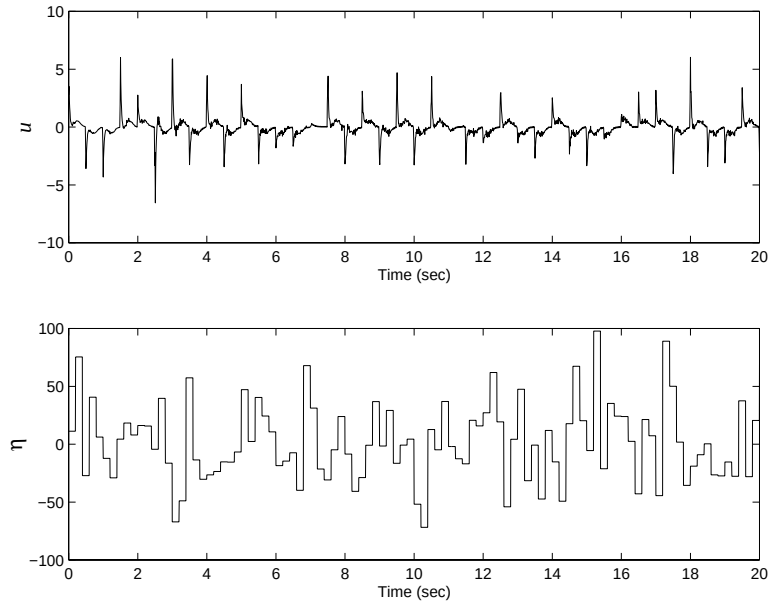

Figure 13: Plot of control effort $u(t)$ and disturbance $\eta(t)$ versus time in Example 2.

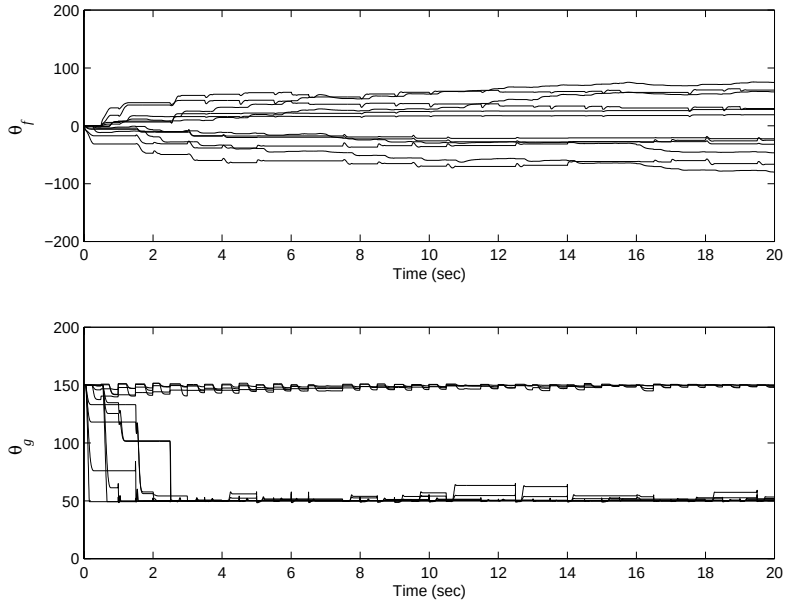

Figure 14: Plots of the components of the parameter vectors $\boldsymbol{\theta}_f$ and $\boldsymbol{\theta}_g$ versus time in Example 2

6 Summary

Fischle and Schröder [4, page 38] observed a major limitation of all existing stable adaptive fuzzy controllers, including the ones proposed by us, is that they were developed for systems with unlimited actuators' authority, that is, for systems with no constraints on the effort level of the actuators. If we are serious about real-life applications of fuzzy adaptive controllers, then the case of the actuators with limited authority has to be rigorously analyzed. Another issue of practical importance is the convergence of the adaptation parameters to their "correct" values. Friedland [5, page 345] states: "One may argue that the failure of a parameter estimate to converge to its correct value is a subsidiary issue as long as the adaptive control works (even with the incorrect parameter estimate). This reasoning might be valid if you can ascertain that the algorithm works for every input to which the system might be subjected. But in most applications the performance of the algorithm is tested only with a limited set of inputs. Satisfactory performance for this set of inputs is not a reliable indicator that its performance will be satisfactory for inputs outside the test set." In the

current state-of-the-art adaptive control algorithms, the convergence of the adaptation parameters is usually ensured through the so called *persistently exciting* inputs to the adaptation algorithms. However, the injection of the persistently exciting signals into the adaptation algorithms may not be feasible in real life applications. Thus, an alternative approach to the issues of the convergence of the adaptation parameters is needed.

In the next stage of this research project we will also consider neural adaptive tracking controllers for uncertain systems. The controllers will be tested on the ground vehicle simulation model that is currently being investigated by us. The controllers' tuning will be performed using genetic algorithms.

References

[1] G. Bartolini, A. Ferrara, and V. I. Utkin. Adaptive sliding mode control in discrete-time systems. *Automatica*, 31(5):769–773, May 1995.

[2] R. A. DeCarlo, S. H. Żak, and G. P. Matthews. Variable structure control of nonlinear multivariable systems: A tutorial. *Proceedings of the IEEE*, 76(3):212–232, March 1988.

[3] S. Drakunov, Ü. Özgüner, P. Dix, and B. Ashrafi. ABS control using optimum search via sliding modes. *IEEE Transactions on Control and Systems Technology*, 3(1):79–85, March 1995.

[4] K. Fischle and D. Schröder. An improved stable adaptive fuzzy control method. *IEEE Transactions on Fuzzy Systems*, 7(1):27–40, February 1999.

[5] B. Friedland. *Advanced Control System Design*. Prentice-Hall, Englewood Cliffs, New Jersey 07632, 1996.

[6] K. Furuta. Sliding mode control of a discrete system. *Systems & Control Letters*, 14(2):145–152, February 1990.

[7] W. Gao, Y. Wang, and A. Homaifa. Discrete-time variable structure control systems. *IEEE Transactions on Industrial Electronics*, 42(2):117–122, April 1995.

[8] T. D. Gillespie. *Fundamentals of Vehicle Dynamics*. Society of Automotive Engineers, Inc., Warrendale, PA, 1992.

[9] S. Hui and S. H. Żak. On discrete-time variable structure sliding mode control. *Systems & Control Letters*, 38(4–5):283–288, 10 December 1999.

[10] U. Kotta. Comments on "On the stability of discrete-time sliding mode control systems". *IEEE Transactions on Automatic Control*, 34(9):1021–1022, September 1989.

[11] J. R. Layne, K. M. Passino, and S. Yurkovich. Fuzzy learning control for antiskid braking systems. *IEEE Transactions on Control and Systems Technology*, 1(2):122–129, June 1993.

[12] Y. Lee, J. Q. Gong, B. Yao, and S. H. Żak. Fuzzy adaptive robust tracking control of uncertain systems. *IEEE Transactions on Fuzzy Systems*, 2000. submitted for publication.

[13] W. C. Lin, D. J. Dobner, and R. D. Fruechte. Design and analysis of an antilock brake control system with electric brake actuator. *Int. J. of Vehicle Design*, 14(1):13–43, 1993.

[14] M. E. Magaña and S. H. Żak. Stabilization of discrete-time dynamical systems via projection method. In *Proceedings of the Twenty-First Southeastern Symposium on System Theory*, pages 305–309, FAMU/FSU College of Engineering, March 26–28, 1989. IEEE Computer Society Press.

[15] G. F. Mauer. A fuzzy logic controller for an ABS braking system. *IEEE Transactions on Fuzzy Systems*, 3(4):381–388, November 1995.

[16] Č. Milosavljević. General conditions for the existence of a quasisliding mode on the switching hyperplane in discrete variable structure systems. *Automation and Remote Control*, 46(3):307–314, August 10, 1985.

[17] P. Myszkorowski and U. Holmberg. Comments on "Variable structure control design for uncertain discrete-time systems". *IEEE Transactions on Automatic Control*, 39(11):2366–2367, November 1994.

[18] S. Z. Sarpturk, Y. Istefanopulos, and O. Kaynak. On the stability of discrete-time sliding mode control systems. *IEEE Transactions on Automatic Control*, AC-32(10):930–932, October 1987.

[19] S. K. Spurgeon. Hyperplane design techniques for discrete-time variable structure control systems. *Int. J. Control*, 55(2):445–456, February 1992.

[20] H. Tian and K. Nonami. Discrete-time sliding mode control of flexible rotor-magnetic bearing systems. *Int. J. Robust Nonlinear Control*, 7(1):609–632, January 1996.

[21] V. I. Utkin. Variable structure systems with sliding modes. *IEEE Transactions on Automatic Control*, AC-22(2):212–222, April 1977.

[22] V. I. Utkin. *Sliding Modes and Their Application in Variable Structure Systems.* Mir Publishers, Moscow, 1978.

[23] W.-J. Wang, G.-H. Wu, and D.-C. Yang. Variable structure control design for uncertain discrete-time systems. *IEEE Transactions on Automatic Control*, 39(1):99–102, January 1994.

[24] A. B. Will, S. Hui, and S. H. Żak. Sliding mode wheel slip controller for an antilock braking system. *Int. J. of Vehicle Design*, 19(4):523–539, 1998.

[25] A. B. Will and S. H. Żak. Antilock brake system modelling and fuzzy control. *Int. J. of Vehicle Design*, 24(1):1–18, 2000.

[26] K. D. Young, V. I. Utkin, and Ü. Özgüner. A control engineer's guide to sliding mode control. *IEEE Transactions on Control and Systems Technology*, 7(3):328–342, May 1999.

[27] X. Yu. Discrete variable structure control systems. *Int. J. Systems Science*, 24(2):373–386, February 1993.

[28] X. Yu and R. B. Potts. Analysis of discrete variable structure systems with pseudo-sliding modes. *Int. J. Systems Science*, 23(4):503–516, April 1992.